

Vlasov dynamics for fermions on phase space lattice

S. Chattopadhyay¹

S.N. Bose National Centre for Basic Sciences, Block-JD, Sector 3, Salt Lake, Calcutta-700091, India

Abstract

Within the framework of stochastic one-body approach a simulation procedure to study the Vlasov dynamics for fermi system on phase space lattice is presented. To deal with fermions on lattice, the phase cell occupancy factors are taken to be either 1 or 0 in accordance with the Pauli exclusion principle. This has significant implications. First, the dynamical evolution does not alter initial temperature of the system and secondly, at finite temperature, the proper statistical behaviour related to the fluctuations over the samples is ensured. This method is applied for two distinct cases viz. the monopole vibration of cold dilute nucleus and the evolution of ring shaped matter distribution at finite temperature in the presence of radial flow. In the latter case, fragment multiplicities are found to be depend on the flow velocity. To check the reliability of the present calculations simulations have been performed with different choices of the grid size.

PACS numbers : 21.65. +f, 24.60.Ky, 25.70.Pq

¹e-mail : shila@tnp.saha.ernet.in

1. Introduction

In recent years, considerable efforts have been made to the study of nuclear dynamics within the framework of stochastic one body theories based on Boltzmann-Uheling- Uhlenbeck (BUU) equation. One of the major goals of such theories is to provide a consistent dynamical picture of fragmentation process near the fermi energy domain. For the understanding of the fragmentation phenomenon at this energy regime, within the mean-field description, one plausible mechanism is to retain the effect of fluctuation in the two body collision term of the BUU equation. Several models and important methods of simulation based on Boltzmann- Langevin (BL) equation is proposed [1]-[15] to incorporate stochasticity in to the deterministic transport equation.

On the formal side, Ayik and Gregoire [1] considered an extension of a one body transport model by incorporating higher order correlations in the equation of motion in a stochastic approximation. Later, in a development of the numerical procedure, the evolution of moments of the phase space density distribution is carried out by calculating the correlation matrices at every time step. This in turn, allows to construct a trajectory or the new phase space density in the ensemble space [2]. In principle, by this manner one can specify the new density uniquely provided an infinite number of multipole moments are taken in to account. But, in practice, the evolution of phase space density is considered in the terms of limited number of multipole moments so that simulation of the reaction dynamics in 3 dimension physical space can be performed (for further details see the review [3]). However, in another approach, Randrup and Rемаud [4] recast essentially the same problem within the framework of Fokker-Planck equation. In this method the stochasticity is directly incorporated into the basic two body scattering process. In the numerical implementation of this method, the phase space density $f(\mathbf{r}, \mathbf{p})$ around a point (\mathbf{r}, \mathbf{p}) is represented on the phase space lattice having elementary volume $\Delta s(=\Delta \mathbf{r} \Delta \mathbf{p} / h^D$, D being the dimension of the physical space). The phase cell occupancy factor $n(\mathbf{r}, \mathbf{p})$ is given as $f(\mathbf{r}, \mathbf{p}) = n(\mathbf{r}, \mathbf{p}) \Delta s$. Due to the individual collisions, net flow of phase space density from one of the elementary cells to the others is considered to be a fluctuating quantity characterised by a Gaussian noise [5]. As a result, in this semi-classical treatment, the change of the phase cell occupancy factor $n(\mathbf{r}, \mathbf{p})$ can occur in a continuous manner so that $n(\mathbf{r}, \mathbf{p})$ may attain a unphysical value either greater than 1 or less than 0. This feature, in one hand, allows us to incorporate efficient algorithm for finding the solution of Vlasov part of the stochastic BUU equation in grid space as described in details in Ref. [7]. On the other hand, one needs a provision for smearing of density forcefully within the neighboring phase cells. Although the application of this lattice model in 3D realistic situation is still a formidable task, it has been however, is rigorously tested for simpler cases [5] and also applied to study the growth of density fluctuation due to the thermal agitation of uniform nuclear matter [6],[7]. Simpler algorithm based on ‘test particle approach’ is also put forward [8] which becomes an important tool of studying different aspects of fluctuation phenomena [9]. In case of heavy-ion collision, this model offer an explanation of the observed large fluctuation in the

projectile and target like masses near peripheral collisions [10]. These apart, within the framework of Vlasov equation some interesting investigation associated with the growth of density fluctuation subjected to a given initial condition has also been reported [11].

Let us concentrate on a particular approach for inclusion of fluctuation within the BUU dynamics as developed in Ref. [13] and [14]. Accordingly, the one body phase space of the system is discretised into separate small cells of size $\Delta\mathbf{s}$ and the ensemble space is generated by \mathcal{N} such samples of phase space. To describe fermions on the phase space lattice, each of the enumerated phase cell (say i) is filled up in such a way that every phase cell (ik) (k run from 1 to \mathcal{N}) is either completely filled or vacant. For a given value of ensemble average occupancy factor $\langle n \rangle_i$ for each i we can fill \mathcal{N} number of boxes by identical particles in different ways provided the value of $\langle n \rangle_i$ is not either 1 or 0. In a broader sense, the underlying process responsible for this typical filling up procedure is known as dichotomic stochastic process. The sample mean and variance of the said fluctuation is given by

$$\langle n \rangle_i = \frac{1}{\mathcal{N}} \sum_{k=1}^{\mathcal{N}} n_{ik} \quad \text{and} \quad \sigma_i^2 = \langle n \rangle_i (1 - \langle n \rangle_i) \quad (1)$$

It is to be noted that relation (1) is *independent* of the size of $\Delta\mathbf{s}$. Another important feature is that, whatever be the simulation method used to study the evolution of phase space density or the occupancy factor $n_i(t)$ eq. (1) always holds. Even if we consider the evolution of hot ($T \neq 0$) fermi gas through Vlasov equation no matter whether spatial uniformity retains or the clusterisation occurs, this statistical criteria is always satisfied separately for every phase cell i . To study the effect of the two body collisions on the evolution of one body phase space density, in semi-classical approximation one usually employs the BUU type collision term to the evolution equation. To account for the fluctuations associated to the individual collisions among the particles a method of simulation is proposed in Ref. [13]. in a consistent manner so that the proper balance between the outflow and the inflow term in the collision part of BUU equation is maintained on the sample average description. As a result, the presence of the collisions change $\langle n \rangle_i(t)$ of the state in a different way (unlike to that provided by the Vlasov equation) so that, at the end $\langle n \rangle_i(t \rightarrow \infty)$ represents a equilibrium situation with certain local (or global) temperature and density (see Ref. [13]). Within this formalism the concept of single or mean trajectory can not be retained. For $\Delta\mathbf{s} \rightarrow 0$ the exact solution of BUU (or the Vlasov) equation is recovered for the average description. However, for the fluctuation, relation (1) always holds which is independent of the choice of $\Delta\mathbf{s}$. This is the key result. As long as we stick to the above mentioned description, namely, the values of phase space occupancy factors are allowed to changes in discrete manner (either from 0 to 1 or from 1 to 0 otherwise) the proper measure of fluctuations over the samples are been maintained throughout. As a consequence, the main effort of the simulation procedure is directed at predicting the proper evolution of the ensemble average occupancy at each phase cell only and to check the consistency, we may compare the simulation results with different choices of $\Delta\mathbf{s}$. Need less to say that as we decrease the size of Δx or

that of (Δp) the storage requirement increases substantially. Moreover, unlike the test particle approach, in our case, we have to consider not only the particle states but also the hole states. As a result the memory requirements increase tremendously with the dimension of the physical space. It is important to note that we treat our occupancy factors n_i as binary numbers which essentially reduces the storage requirements to a certain extent (see [13]). However, to perform a 3D calculation for a realistic situation one have to choose bigger size of both Δx and Δp . Therefore, to find out an optimal values of grid sizes, our strategy is to compare the results with different choices of $\Delta \mathbf{s}$ in 2D. In this situation we have a greater freedom of such choices.

As has already been stressed that, our main concern here is to generate proper evolution of sample average distribution function with reasonable accuracy. For this purpose, therefore, investigation can be persuaded within the framework of Vlasov equation. In addition, it provides an opportunity to explore how reliably the time evolution can be described within our formalism where the occupancy factors can take only two discrete values. As a test case we have already studied the problem of spinodal decomposition of nuclear matter [14]. However, for finite nuclear system one has to check the reliability of this new method.

In order to consider propagation of phase space density distribution we follow Nordheim's approach, which is closely related to the well-known test particle method of solving the Vlasov equation [14]. A filled unit phase cell here is considered to be a particle. The time evolution of these particles can be obtained by the standard leap-frog routine through the following equation

$$\begin{aligned} x_k^i(t + \Delta t) &= x_k^i(t) + \mathcal{C} p_k^i(t), \\ p_k^i(t + \Delta t) &= p_k^i(t) + \frac{\Delta t}{\Delta p} \nabla (\tilde{\mathcal{U}}[\rho(r, t)])_k, \end{aligned} \quad (2)$$

where $\mathcal{C} = \frac{\Delta t \Delta p}{m \Delta x}$.

Here $(\mathbf{x}^i, \mathbf{p}^i)$ represents the co-ordinates of the i th particle in the phase space grid which can take only integer values. It may be noticed that to maintain uniformity of the solution over the position space in the case of free streaming gas one has to choose the value of \mathcal{C} to be unity. Therefore for a given grid size the value of time step Δt remains fixed. This ensures that two particles do not appear in the same spatial cell due to the integer truncation during the evolution. This feature then accounts the proper incorporation of Pauli principle in case of Vlasov propagation of n_i . The importance of this issue has been recently explored [16] by the uses of 'test- particle' procedure. Using a well-controlled Vlasov algorithm, it is revealed that the error which arises primarily due to the improper treatment of Pauli principle, drive the collection of test-particles to a state of classical equilibrium. The manner in which fermions are treated within our formalism such a situation never arise which can be understood as follows. For a temperature $T = 0$, the system is considered to be a statistically pure state so that all samples are identical. Due to the deterministic nature of the Vlasov equation they are remain at

the same state. Because the fluctuation σ_i^2 is always equal to zero for every cell i , the system does not acquire any temperature. The error which arises in the simulation does not however, excite the system to a different temperature. For the calculation of gradient term of the effective potential $\tilde{\mathcal{U}}_i$ in equation (3) we introduce a Gaussian folding function having width σ_r so that

$$\tilde{\mathcal{U}}_i = \frac{1}{\mathcal{N}_g} \sum_j e^{-\frac{(\mathbf{r}_i - \mathbf{r}_j)^2}{2\sigma_r^2}} \mathcal{U}(\mathbf{r}_j) \quad (3)$$

where $\mathcal{N}_g = \sum_j \exp[-(\mathbf{r}_i - \mathbf{r}_j)^2/(2\sigma_r^2)]$, is the normalization constant and is independent of i . The bare potential $\mathcal{U}[\rho(\mathbf{r}_j)]$ on the grid may be calculated by using standard Skyrme interaction as used in earlier calculations [14]. To reduce the truncation error that arises in finding the time development of momenta of the particles on grid a method is invoked in Ref. [14]. To provide better energy conversion one may incorporate this correction in the above algorithm.

In the present paper we apply this method of solving nuclear Vlasov equation in two specific situations. In section 2 we study a typical case of monopole vibration of cold isolated nucleus and in section 3 we study the evolution of hot circular ring in presence of radial flow. In this case, inhomogeneity that resides in the initial state of the system, grows with time which results in the formation of fragments; both of these calculations are performed in 2D physical space. Finally in section 4 we summarize our simulation result.

2. Monopole vibration

In this section we shall present simulation results of monopole vibration of a cold dilute nucleus. To check the reliability of our calculation we repeats our calculation for different choices of grid width Δp and Δx . In this situation we consider the evolution of a single sample at temperature $T = 0$. The phase space distribution of the particles is taken to be spherical in both position and momentum space with radii R_m and P_m so that density profile $\rho(R) = \Theta(R - R_m)$, and the magnitude of P_m is scaled to ηP_F . It is to be noted that at $R = R_m$ the density distribution undergoes a discontinuous jump. However, due to the introduction of the folding function in the expression of effective potential as shown in eq.(3), considerable smoothening in the single particle potential can be ensured. Therefore, the effect of the smooth tail in the matter distribution is automatically taken care of. It may be also mentioned that self-consistency between mean field, within which the particles moves and the density at the initial state cannot be achieved in this manner. In the context of semi-classical approximation, the present problem of monopole vibration can be treated in a consistent way without imposing the scaling approximation of momentum sphere [18]. Within the test particle approach, when the scale parameter η is taken to be either very low or very high compared to unity large oscillations in density can be predicted. On the other hand in case of small oscillation where the value of η is chosen to be close to 1, it is observed that oscillation is dies down very rapidly, as a result the energy in the collective mode is transferred into the random

motion [16],[17]. Therefore, it seems appropriate to direct our study for the case of small oscillations only. For a proper description of initial state at temperature $T = 0$ on grid of finite size, η can not vary in a continuous manner. In particular, for $\Delta p = 58\text{MeV}/c$ and $74\text{ MeV}/c$ we have chosen the values of η to be $\simeq 0.88$ and $\simeq 0.75$ respectively. For a given value of fermi momentum $P_F = 260\text{MeV}/c$, these values of η cannot be made any further closer to 1. Here, we present the simulation for two chosen values of $\Delta x = \frac{1}{3}\text{ fm}$ and 0.5 fm . The time steps Δt as decided through the relation $\mathcal{C} = 1$ mentioned above are different for different choices of Δp and Δx . Accordingly, the values are $\Delta t \simeq 5.4$ (for $\Delta p = 58\text{MeV}/c$, and $\Delta x = \frac{1}{3}\text{ fm}$), 7.1 (for $\Delta p = 58\text{MeV}/c$, and $\Delta x = \frac{1}{2}\text{ fm}$), 4.1 (for $\Delta p = 74\text{MeV}/c$, and $\Delta x = \frac{1}{3}\text{ fm}$), 6.5 (for $\Delta p = 74\text{MeV}/c$, and $\Delta x = \frac{1}{2}\text{ fm}$).

Firstly, we observe that Pauli exclusion principle is obeyed within our simulation procedure or, in other words, no two particles access the same phase cell in their process of evolution for all the studied. This feature may be related to the observation that the symmetry in both the spatial and the momentum distribution of the initial state is preserved accurately throughout the evolution. From the point of view of symmetry argument, this is a stringent case where the full spherical symmetry in 2D should be considered. Hence, all the multipole moments of the said distributions (both for momentum and for position) remain at zero. To get an overall idea about the evolutionary pattern we plot in Fig. 1(a) and (b) the time development of mean square radius of the matter distribution for different values of scale parameter η and for comparison, we also plot the same for different choices of Δx . It is to be noted that for different choices of Δp and Δx we cannot prepare exactly identical states of the nucleus. Consequently, there arises a slight variation in the binding energy and also in the rms radius of the initial state. With $R_m = 6\text{ fm}$ mass number of the nucleus is found to lie within the range 64 ± 2 . Simulation of the Vlasov equation being an initial value problem, the amplitude and the initial phase of the the oscillation in the rms radius (or the density) depend on the shape of the potential profile $\tilde{U}(r)$ of the the initial state. However, the time period of the oscillations for different values of spatial and momentum grid size is seen to be almost the same. As we mentioned above, the error that arises mostly due to the incorporation of the leap-frog routine for finding the time evolution of phase space density does not initiate dissipation. On the other hand, this error may attribute a certain amount of mismatch between the momentum distribution and the profile of the effective potential. As a result the particles those start from one side of the nucleus may leak off from the boundary on the other side of it. The lack of the self-consistency in the initial state partly responsible for such 'evaporation' which is not expected at $T=0$. beyond the time $t=70\text{ fm}/c$, which is of the order of the transit time of the particles, evaporation starts. This feature affects the measurements of r_{rms}^2 . The time average values of this quantity show an upward trend. Hence, to reduce this effect, we set up a criteria namely, the particle which lie beyond a sphere of 10 fm radius are considered to be evaporated, and are not employed in the calculation of r_{rms}^2 . We observe that within time $\simeq 250\text{ fm}/c$, the mass number of the nucleus is reduced by 3-4.5. However, the evaporation rate

reduces considerably as we decrease the size of the spatial grid or the size of the time step.

It is a well-known fact that the energy conservation is not realized very accurately within the particle method for finding the solution of partial differential equation. Apart from some simpler situations, mainly due to the storage problem, it is very difficult to provide a solution of Vlasov equation on phase space lattice incorporating superior methods such as described in Ref. [8]. Although we use phase space grids for description of fermions, but in order to invoke the essential properties of the underlying nature of the fluctuation as given by equation (1), phase space occupancy cannot be changed in a continuous manner. As a result, in spite of our use of large number of particles for description of normal nuclear matter in a unit box, the magnitude of total energy per particle E/A at every time step cannot be preserved very accurately. The error arises mainly due to the truncation of momenta p_i . An upper limit of the estimated error in the measurement of total kinetic energy per particle may be given by $(\Delta p)^2/2m$ which is $\simeq 1.5$ MeV for $\Delta p = 60\text{MeV}/c$. In Fig. 1(c) and (d) we plot the evolution of E/A for different situations. Apart from some fluctuation, within the time of 200 fm/c the error of E/A lies within the 1 MeV. Beyond it the slope of E/A curve rises up further. It is clearly seen that overall slope of this curve decreases as we decrease the time step of the simulation.

2. Fragmentation within Vlasov dynamics

In this section we study the evolution of nuclear matter having a shape of a circular ring in the presence of radial flow at a given finite temperature $T \neq 0$. This particular situation seems to be very appropriate for investigation of the dynamical aspects of fragmentation at central collision. Several theoretical calculations revealed that in later stage of nearly central collision, beyond an energy $\simeq 40$ MeV/A, the post collision nuclear complex takes a shape of a torus [19] and the fragments may appear by the breaking up of such a structure. Using statistical models, investigation has also been performed to provide an quantitative estimate about the size and multiplicities of the fragments and their correlation with kinetic energies [20]. From the more general framework of Boltzmann- Langevin model, such studies have also been carried out in the case of 2D physical space [15]. This shows that due to the presence of strong flow along the transverse direction an elongated ring like structure is formed with larger deposition of matter along the transverse direction and the size or mass of the fragments depends on the speed of stretching of such structure. Thus, the size of the fragments depends on the magnitude of the radial flow. To get a rough idea about the expected outcome from a 3D calculation one may rotate such a two dimensional object around its symmetry axis along the direction of collision. This leads essentially to a bubble like structure. However, the mass around its boundary is definitely not uniform. Along the transverse plane a large deposition of matter having a toroidal shape is expected. Due to the presence of relatively large radial flow in this plane the torus may break quickly into several fragments. To mimic this situation as predicted from our earlier calculation [15], here we consider the evolution of ring like structure in 2D in the presence of radial flow.

In the present cases, we take the value of average density $\langle\rho\rangle$ to be $\frac{1}{2}\rho_0$ which is considered to be uniform within the annular region between two concentric circles of radii 5 fm and 15 fm. For proper statistical description of the initial state at temperature $T \neq 0$ we prepare the samples as described in Ref. [14]. The average occupancy factor $\langle n \rangle_i$ over the sample is taken to be a fermi distribution with an appropriate value of chemical potential $\mu(\langle\rho\rangle, T)$ at a given temperature T . In order to determine the momentum distribution at every spatial cell we prepare a set of 100 samples so that sample variance of the total number of particles at each spatial cell is given by the relation $\sigma^2(N) = \sum_i \langle n \rangle_i (1 - \langle n \rangle_i)$ where the sum is on the momentum state only. Next, these samples are distributed randomly at every spatial cell in such a manner so that the sample average values of the density at every spatial cell within the annular region remains at $\frac{1}{2}\rho_0$ and average momentum distribution is represented by identical fermi distributions as mentioned above. By this manner we can introduce the spatial fluctuations in density of about 10% within each of the samples at temperature $T = 7\text{MeV}$. To incorporate radial flow in the initial state one has to provide a boost to the momentum distribution of every spatial cell i so that the magnitude of the boost momentum is given by mv_{fl} and its direction at every spatial cell is decided through the relation $\tan(\theta_{fl}) = y_i/x_i$.

Let us concentrate on the simulation result. Due to the presence of the radial flow in the initial state, the size of the central hole increases gradually with time. In addition, the spatial fluctuation that resides in the initial state grows with time which leads to the appearance of fragments in the later stages of the evolution. The energy associated with the radial flow is continuously transferred into the internal energy so that the rate of recession decreases gradually. Clusterisation is observed even in the average level of the spatial density distribution. This is a general feature of the evolution that we observe here. To check the reliability of our calculation we have performed our simulation for different values of $\Delta\mathbf{s}$. For the first case, we chose the values of $\Delta p = 58 \text{ MeV}/c$ and $\Delta x = \frac{1}{3} \text{ fm}$ so that the number of particles needed to describe normal nuclear matter within a box of size 1 fm is given by 603 whereas this value is 148 for the choice of $\Delta p = 74 \text{ MeV}/c$ and $\Delta x = \frac{1}{2} \text{ fm}$. In Fig. 2 and 3, we plot the sample average density on the spatial grid at two regimes of the dynamics for two given initial values of flow velocity ($v_{fl} = 0.12c$ and $0.9c$) with the smaller size of $\Delta\mathbf{s}$. Initial transients in the density fluctuations (Fig. 2(a) and 3(a)) ultimately lead to a steady pattern. The clustered nature of this pattern (Fig. 2(b) and 3(b)) yields evidence of the trend towards fragmentation. Later on, the relative distance between the clusters gradually increases. It is also to be noted that similar such patterns are also observed in our simulation for other choices of $\Delta\mathbf{s}$. The crucial role of the initial flow on this pattern is evident from these figures. Fragmentation starts after this steady pattern appears in the matter distribution. Therefore, one may safely guess at the average number of the fragments produced. To identify fragments in every individual sample we use the ‘spanning tree method’ where we take the boundary of a fragment on the spatial grid to extend to the point where matter density reaches a value lower than $0.11\rho_0$.

The mode of fragmentation can be split into two distinct regime. Firstly, due to the continuous stretching fluctuations grows to a certain extent, so that the ring shaped structure initially breaks up with at least one large chunk which very quickly undergoes fragmentation. The average size or the mass of such clusters is determined by the initial conditions, primarily the magnitude of the flow velocity v_{fl} . Later, due to evaporation the mass of the fragments reduces steadily. Although the time scale of the fragmentation process depends crucially on v_{fl} and also on temperature, these distinguishing features of the dynamics are present in every case, this can easily be recognised from the study of time evolution of fragment mass abundances. To quantify, in Fig. 4 we plot the frequency distribution versus fragment mass at different times for 100 samples. To make a direct comparison, the time evolution of fragment mass abundances for two distinct cases are shown in the same panel. Depending upon the initial values of v_{fl} this distribution peaks around two different values of mass number. Even at early stages of the fragmentation, we observe this characteristic feature of the dynamics. However, because of evaporation both the peaks shift towards smaller values of mass number in course of time. It is to be mentioned that we could not provide a proper description of the production of light particles such as proton, neutron, deuteron, triton etc. In the current scheme even more than 30% of the initial mass simply evaporated out at the earlier stages of the evolution (when production of such particles is expected) without producing any fragments. To get an idea about how far we can rely on our calculation for the details of the fragmentation dynamics, in Fig. 5 and 6 we compare our results on time evolution of mass abundances that are shown in Fig. 4 with the same data which are extracted from the simulation with other choices of Δs . As we increase the grid size, the rate of evaporation increases. Apart from this, the nature of the spectra does not change which can also be seen from the plot of cumulative frequency versus fragment mass given in Fig. 6 for higher values of v_{fl} . To get an idea about the promptness of the fragmentation process, we plot the time evolution of average number of fragments per sample in Fig. 7. The time beyond which fragments appear, is defined as the onset time t_{onset} . Beyond this time, the number of fragments per sample ultimately saturates to a certain steady value. The time that is needed to reach this saturation (in other words the fragmentation time t_{frag}) can be estimated from this curve. For $v_{fl} = 0.12c$ the estimated value of $t_{frag} \simeq 50\text{fm}/c$ which is quite small in comparison to the value of $t_{onset}(\simeq 125\text{ fm}/c)$. For lower values of v_{fl} , one has to wait for a much longer time $\simeq 200\text{ fm}/c$ to observe fragments. In this case, it is observed that the estimates of t_{onset} as well as the total number of fragments changes only to be slightly for different choices of Δs .

4. Summary

In order to treat fermions in the same way as provided by the Boltzmann - Langevin model, we introduce in this paper a simulation method of Vlasov dynamics on phase space lattice. This simulation procedure is designed in such a manner that the Pauli principle can be ensured very accurately and proper statistical criteria related to the fluctuation of phase space density (as given by eq.(1)) can be

fulfilled. This becomes an important issue, specially, for the study of growth of fluctuations in hot fermi systems. In the context of Vlasov dynamics, this feature guarantee an evolution of isothermal samples. For illustration of this method we consider two specific cases namely; monopole vibrations of a cold dilute nucleus and the evolution of ring shaped matter distribution in the presence of thermal noise.

For the first case, it is observed that within our simulation scheme, the symmetry that resides in the initial state of the spherical nucleus is preserved under Vlasov propagation of phase space density. This result is verified further from the simulation with different choices of phase cell size Δs . However, in spite of our use of a large number of particles for simulation, the magnitude of total energy per particle of the system can not be retained with enough accuracy. The problem mainly arises due to the application for large time step of the leap-frog routine. In order to provide an energy conserving evolution we can not take the most obvious option (as adopted in the test particle approach of simulation) of choosing the time step to be arbitrarily small. In such cases we invariably face the problem of incorporating pauli principle in the dynamics.

It is to be noted that at zero temperature, the system is defined uniquely by a single trajectory (or sample). On the other hand, in case of finite temperature, one needs a collection of samples for proper description of the system to a certain accuracy one needs a collection of samples, the degree of which should increase with the size of the collection. In this situation, the concept of a single or mean trajectory does not make any sense. The initial fluctuations in density within the samples arises solely due to thermal agitation. If we consider a situation of thermal equilibrium, the amplitude of the density fluctuations is decided by the magnitude of temperature and sample average density. Within our method of simulation, it becomes possible to provide a proper description of noise consistent with the average properties of the system even at time $t = 0$. Within the Boltzmann-Langevin model, because of the presence of the fluctuation collision term (or the source term) the details of the evolution do not depend very much on how one prepare the initial samples. The fluctuations associated with the initial state may appear in a additive manner to the dynamics which presumably, cannot be true in the case of Vlasov dynamics. Due to the deterministic nature of the evolution, the inhomogeneity that exists initially within every sample, develops independently with time. To asses its role in the dynamics, an investigation was carried on by the authors of Ref [11]. Using a very accurate algorithm for the simulation of Vlasov equation they found that the neighbouring particle trajectories diverge exponentially with time, concluding, that the associated dynamics may be characterised by classical noise. As the situation demands, we perform our simulation with a different initial temperature of 3.5MeV. Although the essential features remains to be unaltered as seen by the observation of the similar evolutionary pattern (as given by Fig. 2 and 3.), however, the fragments appear very late in time. For $v_{fl} = 0.12c$, the onset time of the fragments takes a value $\simeq 200\text{fm}/c$. We also repeat our calculations with different sets of initial samples. The observed differences may arise due to the fact that the sample sets that are prepared with different choices of Δs

are not identical.

In a realistic situation of ion-ion collision, the formation of structure of toroid shape has been predicted in different calculations. The usual statistical models that are employed to study the fragmentation of a hot residue has no provision to consider the dynamical features of collective radial flow. Within a less complicated scenario of two dimension, we investigate the role of radial collective flow on the dynamics of fragmentation of circular ring, a 2D counterpart of the torus. We also emphasis on the fact that the results of our simulation does not depend on the choices of grid size. This is an important aspect, as otherwise, one can not provide a proper estimate of fragment multiplicities from a dynamical calculation.

References

- [1] S. Ayik and C. Gregoire, Nucl. Phys. **A513**, 187 (1990); Phys. Lett. **B212** 269 (1988).
- [2] E. Suraud, S. Ayik, M. Belkacem and J. Stryjowski, Nucl. Phys. **A542**, 141 (1992), E. Suraud, S. Ayik, M. Belkacem and F.S. Zhang, Nucl. Phys. **A580**, 323 (1994).
- [3] Y. Abe, S. Ayik, P.G. Reinhard and E. Suraud, preprint, (Yukawa Inst. Kyoto) YITP-95-18 (1995).
- [4] J. Randrup and B. Remaud, Nucl. Phys. **A514**, 339 (1990).
- [5] Ph. Chomaz, G.F. Burgio and J. Randrup, Phys. Lett. **B254** 340 (1991); G.F. Burgio, Ph. Chomaz and J. Randrup, Nucl. Phys. **A529**, 157 (1991); G.F. Burgio, B. Benhassine, B. Remaud and F. Seville, Nucl. Phys. **A567**, 626 (1994).
- [6] G.F. Burgio, Ph. Chomaz and J. Randrup, Phys. Rev. Lett. **69**, 885 (1992); M. Colonna, Ph. Chomaz and J. Randrup, Nucl. Phys. **A567**, 637 (1994).
- [7] G. F. Burgio, Ph. Chomaz, M. Colonna and J. Randrup, Nucl. Phys. **A581**, 356 (1995).
- [8] M. Colonna, G.F. Burgio, Ph. Chomaz, M. Di Toro and J. Randrup, Phys. Rev. C **47**, 1395 (1993).
- [9] M. Colonna, M. Di Toro, A. Guenera, V. Latora and A. Smerzi, Phys. Lett. **B307**, 273 (1993). M. Colonna, M. Di Toro and A. Guenera, Nucl. Phys. **A580**, 312 (1994); M. Colonna, and Ph. Chomaz, Phys. Rev. C **49**, 1908 (1994); A. Guenera, M. Colonna and Ph. Chomaz, Phys. Lett. **B373**, 267 (1996).
- [10] M. Colonna, M. Di Toro, A. Guenera, V. Latora, A. Smerzi and Z. Jiquan, Nucl. Phys. **A583**, 525c (1995).
- [11] G.F. Burgio, M. Baldo and A. Rapisarda, Phys. Lett. **B321**, 307 (1994); M. Baldo, G.F. Burgio and A. Rapisarda, Phys. Rev. C **51**, 198 (1995).
- [12] G. F. Burgio, Ph. Chomaz and J. Randrup, Phys. Rev. Lett. **73**, 3512 (1994).
- [13] S. Chattopadhyay, Phys. Rev. C **52**, R480 (1995).
- [14] S. Chattopadhyay, Phys. Rev. C **53**, R1065 (1995).
- [15] S. Chattopadhyay, preprint, nucl-th/9603038 (1996).
- [16] P.G Reinhard and E. Suraud, Anns. Phys. (N.Y) **239** 193 (1995).
- [17] C. Jarzynski and G.F. Bertsh, Phys. Rev. C **53**, 10228 (1996).

- [18] D.M. Brink, A. Dellafiore and M. Di Toro, Nucl. Phys. **A456**, 205 (1986).
- [19] W. Bauer, G.F. Bertsch and H. Schulz, Phys. Rev. Lett. **69**, 1888 (1992); H.M. Xu, C.A. Gagliardi, R.E. Tribble and C.Y. Wong, Nucl. Phys. **A569**, 575 (1994).
- [20] L. Phair, W. Bauer and C.K. Gelbke, Phys. Lett. B **314**, 271 (1993); T. Glasmacher, C.K. Gelbke and S. Pratt, *ibid.*, 265 (1993); Subrata Pal, S.K. Samaddar, A. Das and J.N. De, Phys. Lett. B **337**, 14 (1994).

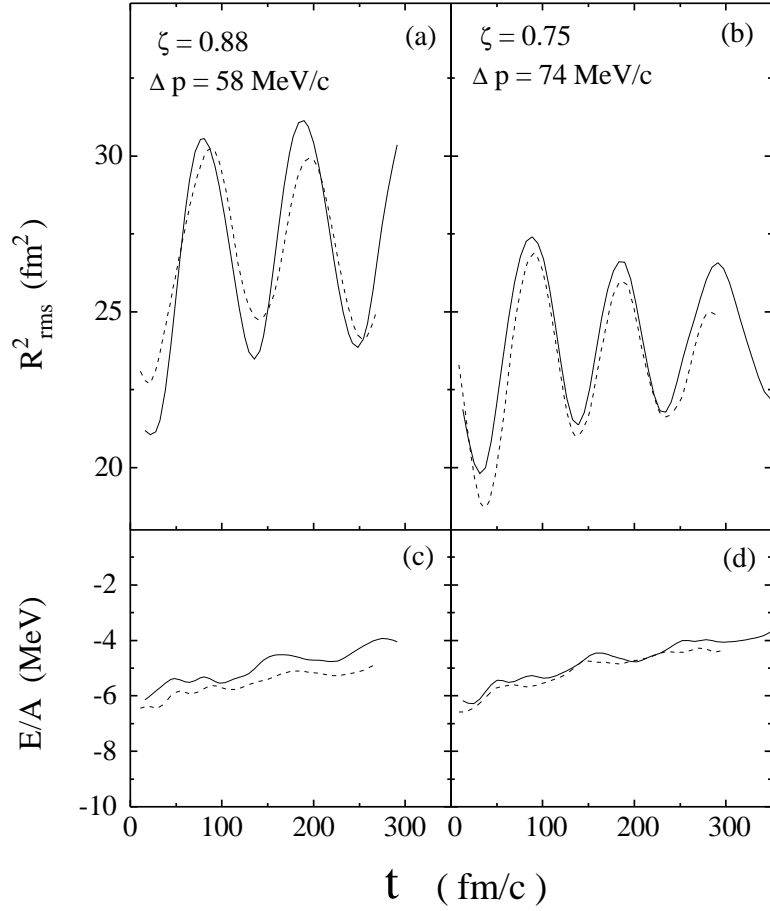


Fig. 1

Time evolution of mean square radius r_{rms}^2 and energy per particle E/A of monopole vibration of an isolated nucleus is shown for different values of momentum scale factor η . The solid and dotted curves represent the simulation results with $\Delta x = \frac{1}{3}$ fm and $\frac{1}{2}$ fm respectively.

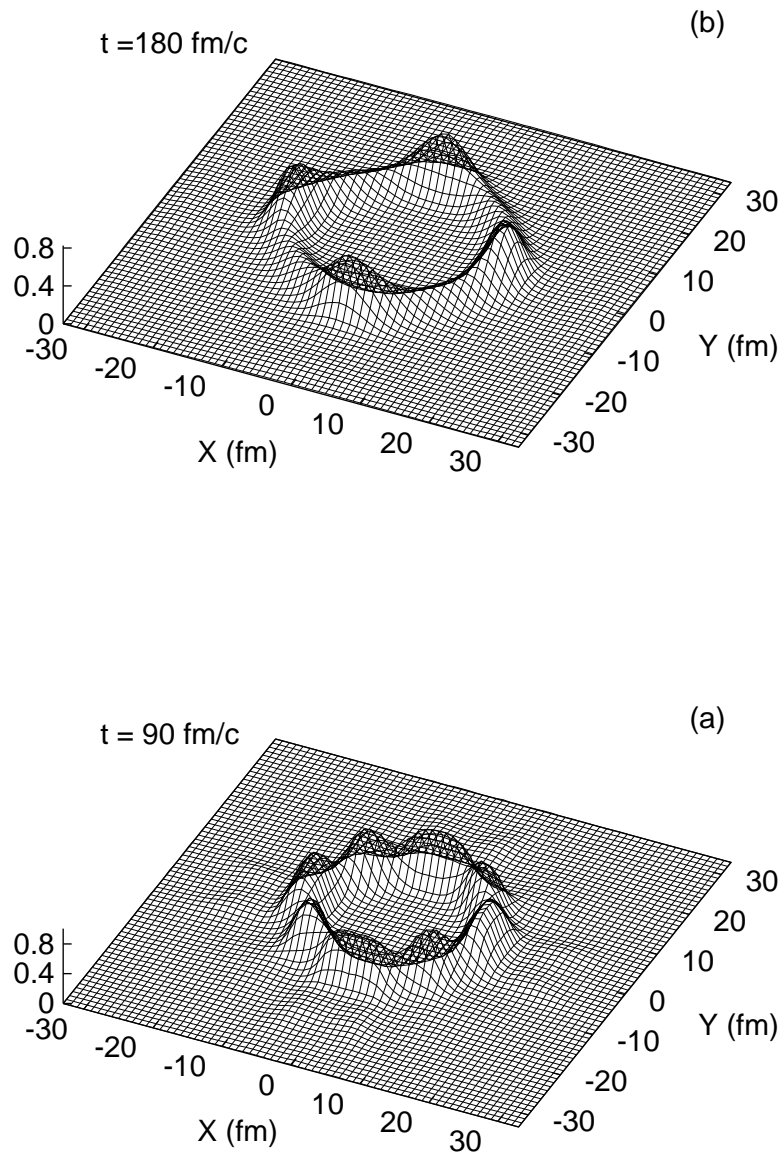


Fig.2

Spatial variation of the sample averaged density distribution $\langle \rho(x, y; t) \rangle$ in unit of ρ_0 is exhibited for the initial flow velocity $v_{fl} = 0.09c$. The simulation results are with $\Delta p = 58 \text{ MeV}/c$ and $\Delta x = \frac{1}{3} \text{ fm}$.

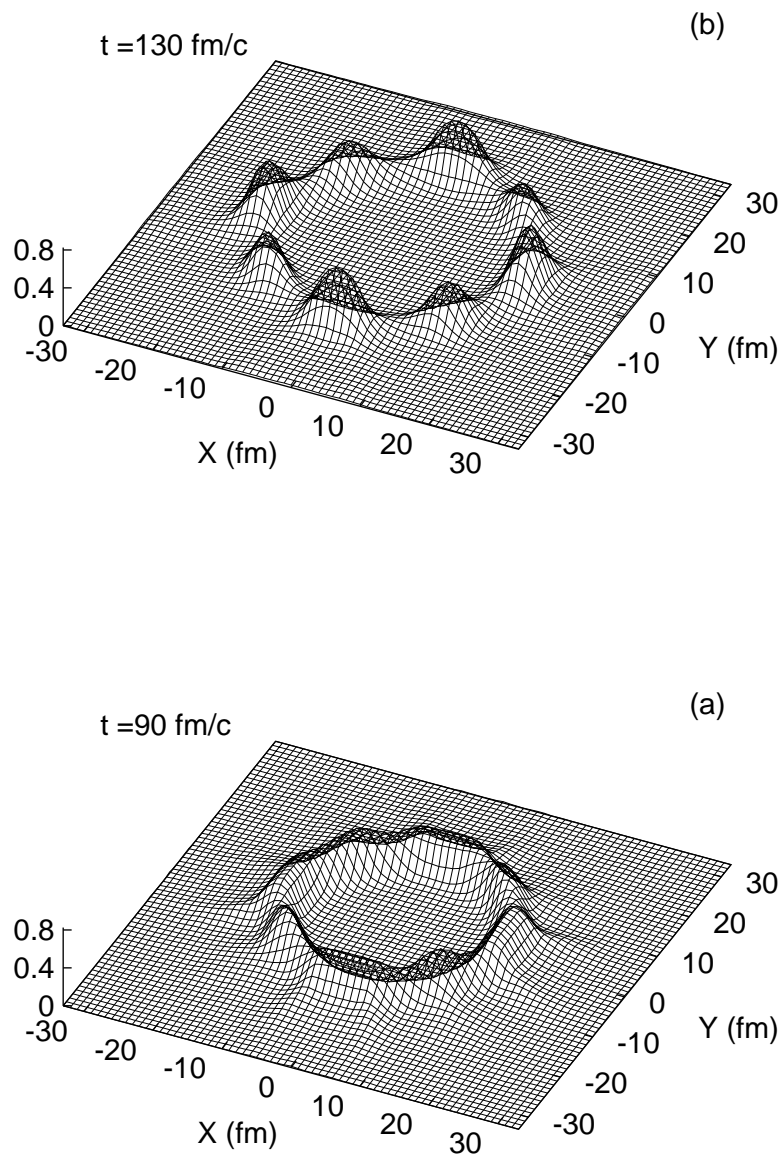


Fig.3

Same as that of Fig. 2 with $v_{fl} = 0.12c$.

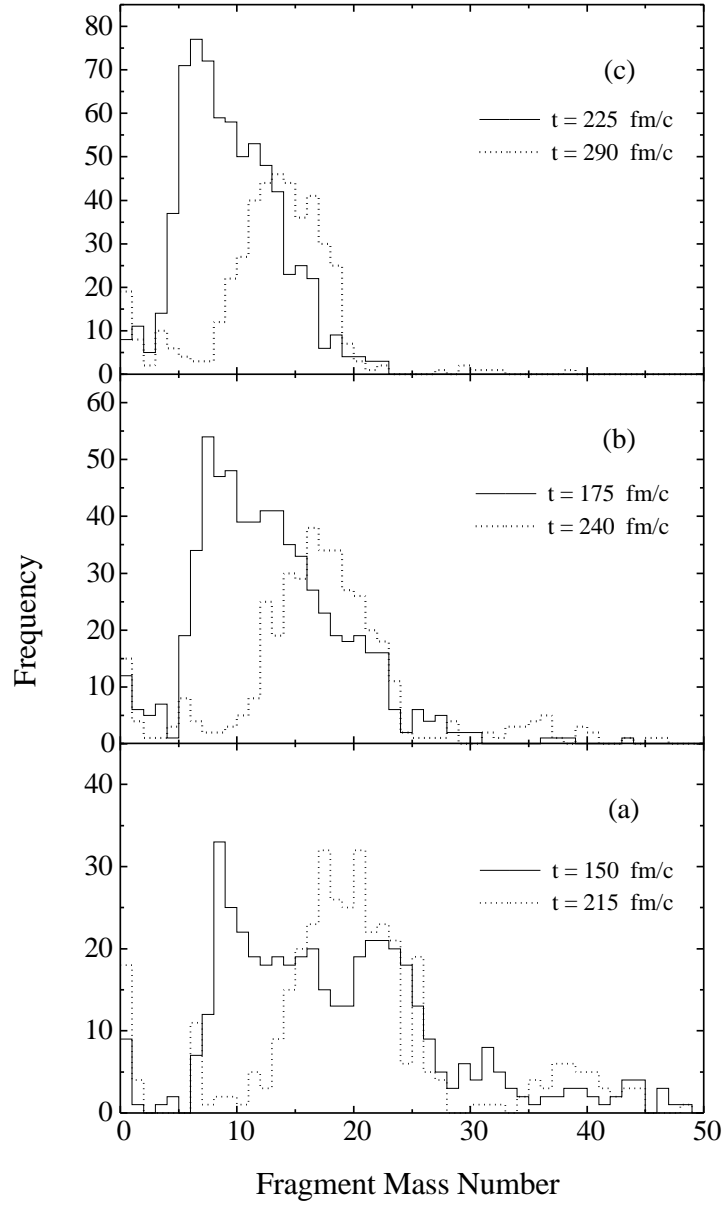


Fig.4

Time evolution of fragment mass abundances are plotted for two different values of initial flow velocity $v_{fl} = 0.12c$ (solid histogram) and $0.09c$ (dotted histogram). Simulation results with $\Delta p = 74$ MeV/c and $\Delta x = \frac{1}{2}$ fm are shown for different times in panels (a)-(c).

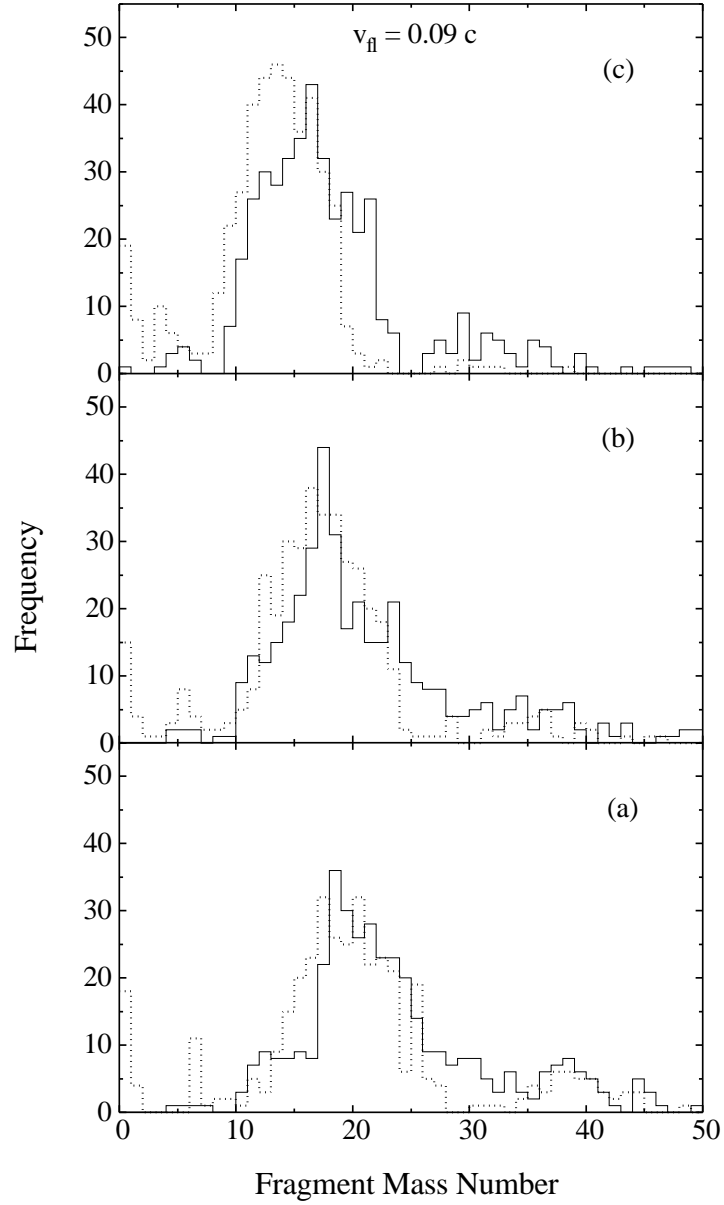


Fig.5

Time evolution of fragment mass abundances for $v_{fl} = 0.09c$ shown by dotted histogram in Fig. 4 are compared with that calculated from the simulation with the choice of $\Delta p = 58 \text{ MeV}/c$ and $\Delta x = \frac{1}{3} \text{ fm}$ (shown by solid histogram).

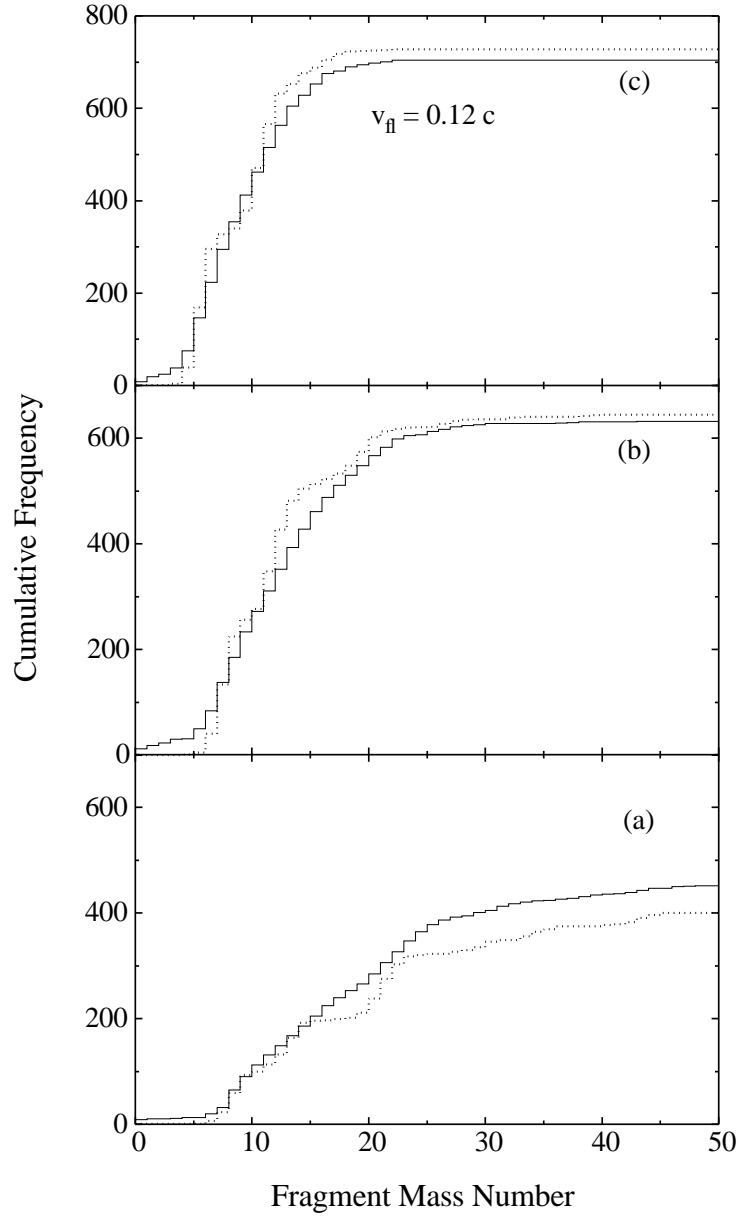


Fig.6

The cumulative frequency versus fragment mass number is plotted for different times. Solid histogram represents the same data as shown for initial values of $v_{fl} = 0.12c$ in Fig.4 which are compared with the calculated results from the simulation with the choice of $\Delta p = 58 \text{ MeV}/c$ and $\Delta x = \frac{1}{3} \text{ fm}$ (shown by dotted histogram).

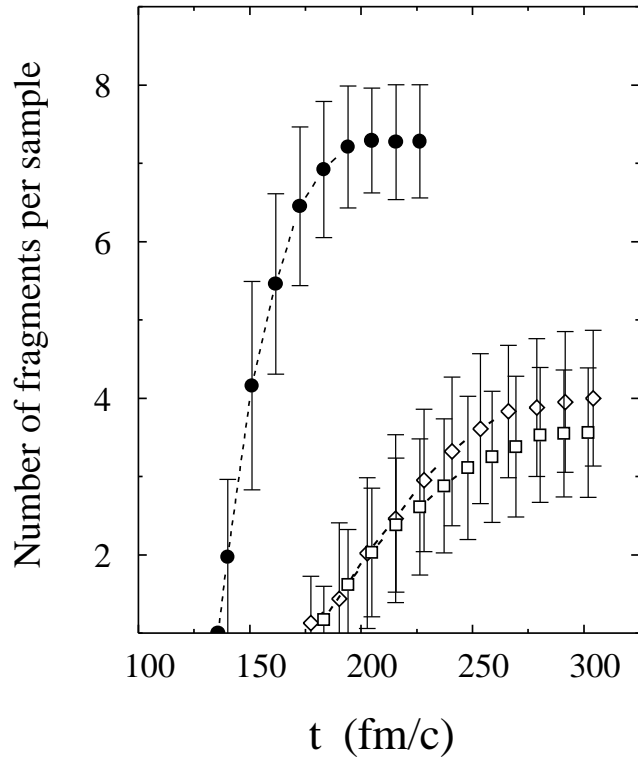


Fig.7

Time evolution of average number of fragments per sample for two given values of $v_{fl} = 0.12c$ and $0.09c$ are shown by solid and open points. The open square and open box represent the simulation results for two given choices of Δs , ($\Delta p = 74 \text{ MeV}/c$, $\Delta x = \frac{1}{2} \text{ fm}$) and ($\Delta p = 58 \text{ MeV}/c$, $\Delta x = \frac{1}{3} \text{ fm}$) respectively. The sample fluctuations are indicated by the error bars. The curves connecting the points are to guide the eye.